HERCULES

High-Temperature Thermochemical Heat Storage
Powered by Renewable Electricity
for Industrial Heating Applications

Deliverable D2.3: Chemical kinetics model of the redox material

Dissemination Level: PU

HORIZON-CL5-2022-D4-01-05

Project No: 101104182

Funded by
the European Union

DELIVERABLE FACTSHEET

Deliverable D2.3	
Work Package	2
Work Package Leader	Centre for Research & Technology Hellas (CERTH)
Deliverable Title	Chemical kinetics model of the redox material
Dissemination Level	Public
Due date of the Deliverable:	M21 - 28.02.2025
Actual Submission Date:	M21- 28.02.2025
Author(s):	Michalis Mouratidis, Chrysa Pagoura, George Karagiannakis
Contributor(s):	Nickolas Vlachos
Reviewer(s):	Christos Agrafiotis (DLR)

All rights reserved: The document is proprietary of the HERCULES consortium members. No copying or distributing, in any form or by any means, is allowed without the prior written agreement of the owner of the property rights. Funded by the European Union. Views and opinions expressed are however those of the author(s) only and do not necessarily reflect those of the European Union or the European Climate, Infrastructure and Environment Executive Agency (CINEA). Neither the European Union nor the granting authority can be held responsible for them.

Contents

Tables

Figures

1 Introduction

The present deliverable details the oxidation and reduction kinetics modeling activities of the perovskite material using experimental data from thermogravimetric analysis (material in powder form; e.g. see submitted deliverable D1.2) and in a temperature-programmed electrical furnace in which small-scale structured bodies were used (e.g. see deliverables D1.3 and D2.1. D2.2).

The determination of chemical kinetics is vital for understanding the perovskite behavior under different process conditions and as a result a useful tool towards process design definition and optimization. In order to study the perovskite chemical kinetics, the perovskite with the best performance was opted, based on the laboratory experiments in small-scale structured bodies carried out within the project so far. The experimental results indicated that the perovskite composition with the best performance is the $Ca_{0.9}Sr_{0.1}MnO_3$, which will be mentioned as CS10MO in this deliverable.

In later stages of the project, the developed kinetic model will be coupled with a CFD model to carry out realistic simulations of the process and contribute towards scale up process design. Moreover, the kinetic model will also be adjusted to the case of $CaMn_{0.875}Al_{0.125}O_3$ (CMA12O) as soon as relevant structures are shaped and evaluated. The present deliverable defines a first complete version of the model, which will be continuously refined as additional experiments will become available and also considering the needs of WP3 studies.

2 Experimental data

The oxidation and reduction reaction kinetics were investigated within the temperature range of 600 and 1350 K (~ 300-1100°C) using both air and inert gas. Information from two experimental configurations were used; a thermogravimetric analysis (TGA) instrument (as already described in D1.2) and an in-house lab scale furnace/purpose-built test-rig (see D2.1).

The two experimental configurations were capable to provide useful information with different characteristics. The TGA is performed with mg-scale quantities of redox material powder, in which various heating protocols and atmospheres can be used while measuring the weight loss of the sample with increased accuracy. In the electrical furnace experiments carried out with the aid of a purpose-built test-rig, larger perovskite structures can be utilized. Various atmospheres as well as heating and pressure protocols can be applied, while measuring the oxygen concentration at the outlet during the redox process.

The test-rig experiments may provide lower accuracy of the measured oxygen released by the structure. Low oxygen release – which takes place at low temperatures (i.e. close to 750°C) – may be insignificant when compared to the amount of oxygen present in the air. However, it is suitably designed to perform experiments with larger structures which is more indicative to the real process conditions.

In both experimental configurations, the experimental data were related to the non-stoichiometry factor, δ, as it is described in the following section.

3 Cyclic reduction-oxidation (redox) reaction theoretical approach

The perovskites intend to store heat via a hybrid chemical-sensible storage concept. The sensible part refers to the increase or decrease of the structure's sensible temperature. The chemical part refers to the material reduction and oxidation reactions that can absorb or release thermal energy due to the associated reaction enthalpy, according to the process conditions. This reaction exhibits an oxygen non-stoichiometry that is represented by a parameter, δ (-) (Bulfin et al., 2020). For instance, for a CS10MO perovskite, the redox operation can be described by a forward and a backward reaction (de Diego et al., 2014) according to the following reversible scheme:

$$Ca_{0.9}Sr_{0.1}MnO_3 \rightleftharpoons Ca_{0.9}Sr_{0.1}MnO_{3-\delta} + 0.5 \cdot \delta \cdot O_2 + \Delta H_{RXN}$$

The non-stoichiometry parameter δ is defined as the number of atomic oxygen molecules released divided by the number of molecules of the perovskite (powder or structure) participating in the redox scheme. The parameter δ is considered to be the decisive parameter of redox operation. From experiments carried out in WP2, it has been concluded that δ can vary at least with changes in temperature, pressure and oxidizer (i.e. O_2) molar fraction. By definition, the non-stoichiometry parameter δ can be described with the equation below:

$$\delta\left(T, p, Y_{O_2}\right) = \frac{mol_{O,released}}{mol_{perovskite}} = \frac{mass_{perov}\left(T_{ref}, p_{ref}, Y_{O_2,ref}\right) - mass_{perov}\left(T, p, Y_{O_2}\right)}{mass_{perov}\left(T_{ref}, p_{ref}, Y_{O_2,ref}\right)} \frac{MW_{perov}}{MW_O}$$

Where T is the temperature on the surface of the material in K, p is the operating pressure in Pa, Y_{O_2} is the oxygen molar fraction in the atmosphere (-), MW is the molecular weight in kg/mol and $mass_{perov}$ is the perovskite mass in kg.

3.1 Model assumptions

In order to model the redox reaction kinetics, perovskite behavior as recorded during the TGA and test-rig experiments was analyzed. Based on the experimental findings, certain assumptions were made so as to formulate the redox kinetic model.

During the experiments, the perovskite structure was considered to have uniform temperature throughout its volume. This assumption is valid for the TGA experiments – in which perovskite powder is used –but is less accurate for the test-rig experiments. Therefore, in order to export the kinetic parameters, TGA measurements were taken into consideration. On the other hand, experimental data from the test-rig was utilized for model predictions verification, accepting the error imposed by any thermal gradients. A coupled kinetic-thermal model will be implemented via the coupled kinetic CFD model in the frame of WP3 activities and is beyond the scope of this deliverable.

It has been observed that, at isothermal conditions, δ reaches an equilibrium relatively fast, which indicates that the two competitive reduction and oxidation reaction rates become equal after a while. Additionally, at different isothermal conditions δ reaches also different equilibrium levels. It has been assumed that these phenomena are attributed to the fact that while δ is being increased, further material reduction becomes more and more difficult, whereas the opposite is true for the oxidation.

As a result, increasingly more energy is required in order to subtract oxygen molecules from the structure, while the reduction progress enhances the material ability to regain oxygen molecules.

Another effect to be considered is the intrinsic characteristics of the perovskite. Except for the macropores – from which gas can flow easily – the material itself has also micron-to-nano-sized pores through which oxygen molecules can migrate. During the experiments, both material powder and structure with wall thickness up to a few millimeters were examined. It has been observed macroscopically that the effect of wall thickness was small if not negligible, therefore intrinsic characteristics were not considered by the model. However, further studies will be carried out to determine the significance of thicker walls intrinsic characteristics.

Oxidation and reduction steps are considered to be two competitive phenomena that can take place simultaneously during both reduction and oxidation processes. Depending on the operating conditions (temperature, oxygen molar fraction, value of δ at any given moment), either of the two reactions will be favored resulting to the overall material reduction or oxidation. This work has studied the oxygen molar fraction effect on the redox progress, albeit not yet to its full extent. Except for experiments carried out under air, perovskites were tested under flows with different oxygen molar fractions. It has been assumed that oxygen molar fraction affects only the oxidation reaction. The level of the effect of oxygen molar fraction on the redox reactions has been preliminarily studied and further work will be performed during the course of the project. Last but not least, operating pressure has not been considered by the model as it is beyond the scope of HERCULES concept.

3.2 Model mathematical formulation

Given the above model assumptions, it can be argued that a reduction and an oxidation reaction take place, which can be described from Eq. 1 to Eq. 4 . The two reactions are considered to follow the Arrhenius Law (Go et al., 2008), in which the activation energy was not assumed as constant. Instead, activation energy is directly affected from the value of δ. The set of equations below can mathematically describe the above considerations.

$$\text{Reduction}: \left.\frac{d\delta(t)}{dt}\right|_{red} = Rate_{red} = k_{0_{red}} \exp\left(-\frac{E_{A,red}}{R\,T}\right) \quad \text{Eq. 1}$$

$$E_{A,red} = E_{A,0,red} + c_{red}\,\delta^{\delta exp_{red}} \quad \text{Eq. 2}$$

$$\text{Oxidation}: \left.\frac{d\delta(t)}{dt}\right|_{ox} = Rate_{ox} = -\,k_{0_{ox}}\,{Y_{ox}}^{yexp}\,\exp\left(-\frac{E_{A,ox}}{R\,T}\right) \quad \text{Eq. 3}$$

$$E_{A,ox} = E_{A,0,ox} - c_{ox}\,\delta^{\delta exp_{ox}} \quad \text{Eq. 4}$$

Where k_0 [s^{-1}] is the pre-exponential factor, Y_{ox} [mol_{O2} mol_{gas}^{-1}] is the instantaneous oxygen molar fraction in the process gas, E_A [J mol^{-1}] the activation energy, R [J mol^{-1} K^{-1}] is the gas constant, T [K] is the substrate temperature, $E_{A,0}$ [J mol^{-1}] is the activation energy at low temperatures or at zero δ

values and c [J mol^{-1}] and δexp [-] are constants that correlate the effect of δ on the activation energy.

4 Parameter estimation

The estimation of the kinetic parameters, based on the given mathematical equations, was achieved using experimental data from TGA studies. Optimization algorithms within gPROMS software environment have been used in order to calculate the parameters, through resolution of a minimization problem. The latter involves an objective function to minimize the error between model predictions and experimental results. This maximizes the probability that the mathematical model will predict the measurement values obtained from the experiments.

It is important to feed appropriate experimental data so as the algorithm is capable to produce reliable results. Although there are a few studies reporting perovskite redox kinetics, they adopt different approaches. Therefore, there is some uncertainty regarding the order of magnitude of these parameters, a fact that complicates the estimation procedure.

In this work, steps have been taken, described in the following sections, to facilitate the estimation procedure by separating mechanisms and using mathematical simplifications.

4.1 Reduction kinetic parameters

It is possible to experimentally isolate the reduction mechanism from the oxidation one by increasing the substrate temperature under inert (i.e. no presence of oxygen) atmosphere. This was achieved in a special-designed TGA experiment. Nitrogen with a purity of 99.999% was fed into the chamber for half an hour prior to the initiation of material reduction. After this time, the temperature was increased in a stepwise manner, starting from 873 K (600 °C) up to 1273 K (1000 °C) and performing an isothermal step every 50 K with a dwell time of 15 min at each temperature. Between the isothermal steps, a heating rate of 10 K/min was applied and the sample was heated up to 1273 K (1000°C). Then, the gas was changed to air to initiate the oxidation process, cooling the substrate under the same step-wise temperature-time profile down to 673 K (400°C). This procedure was repeated twice, as it is shown in Figure 1.

It is observed that in the second repetition a lower maximum δ value was achieved at the highest temperature. This indicates that the small amount of oxygen still existing in the chamber – due to the fact that the chamber was purged with nitrogen for less time – affected the result. This proves the sensitivity of the material to oxidation, taking place even in very low oxygen concentrations. This finding is also in agreement to relevant results, presented in deliverable D2.1, with structured bodies using the electrical furnace/purpose-built setup. For the parameter estimation procedure the first reduction-oxidation set was considered. Furthermore, it is evident that during the reduction under inert gas, δ does not reach an equilibrium even after 15 minutes of isothermal operation. Naturally, this is proof that, upon consideration of the respective isothermal conditions under air flow, the additional material reduction is largely stopped by the competitive oxidation reaction, as under the presence of excess oxygen δ reaches an equilibrium in less than 30 s during such isothermal operation.

The resulted kinetic parameters for the reduction mechanism are $k_{0,red} = 3.05 \cdot 10^{17}\ s^{-1}$, $E_{A,0,red} = 332000\ J\ mol^{-1}$, $c_{red} = 492000\ J\ mol^{-1}$ and $\delta\exp_{red} = 0.6$. The comparison of the model predictions with the TGA results is shown in Figure 2.

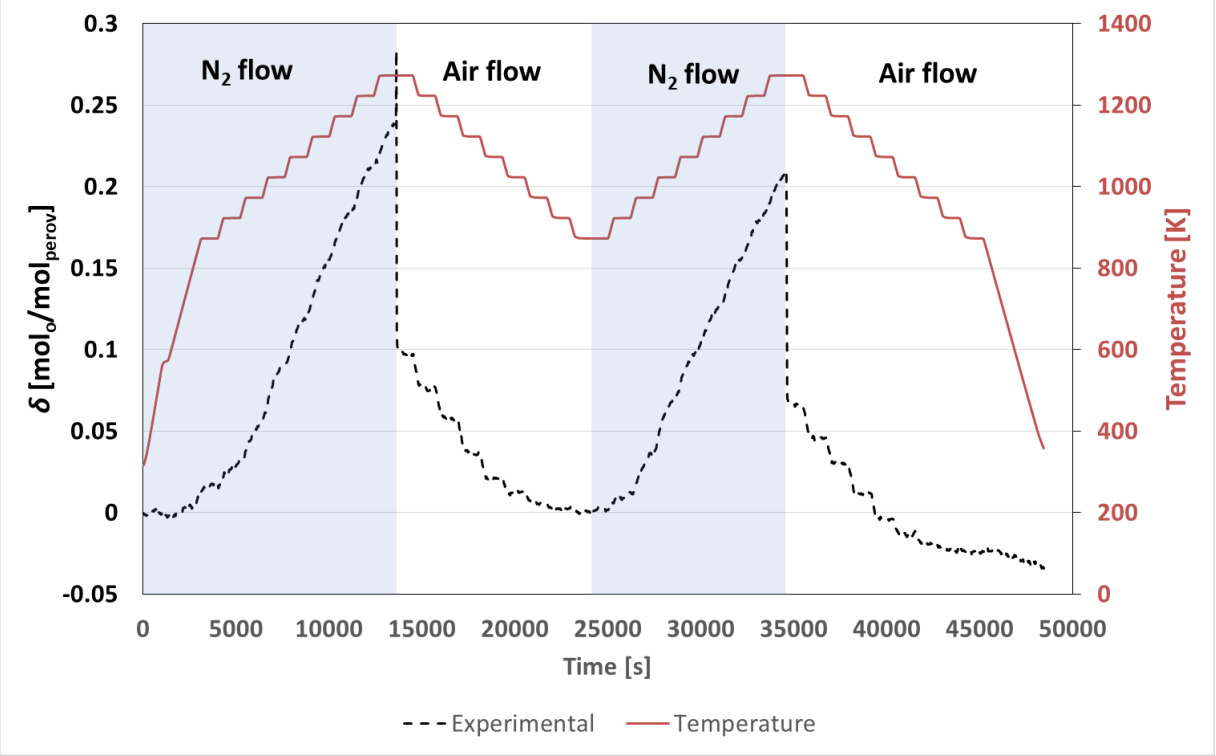

Figure 1: Information from the TGA experiment. Reduction of the material was achieved by heating the sample in a stepwise manner from 873 K up to 1273 K under nitrogen flow. Gas was switched to air and the sample was oxidized in the same stepwise manner by cooling down to 873 K. The procedure was repeated twice.

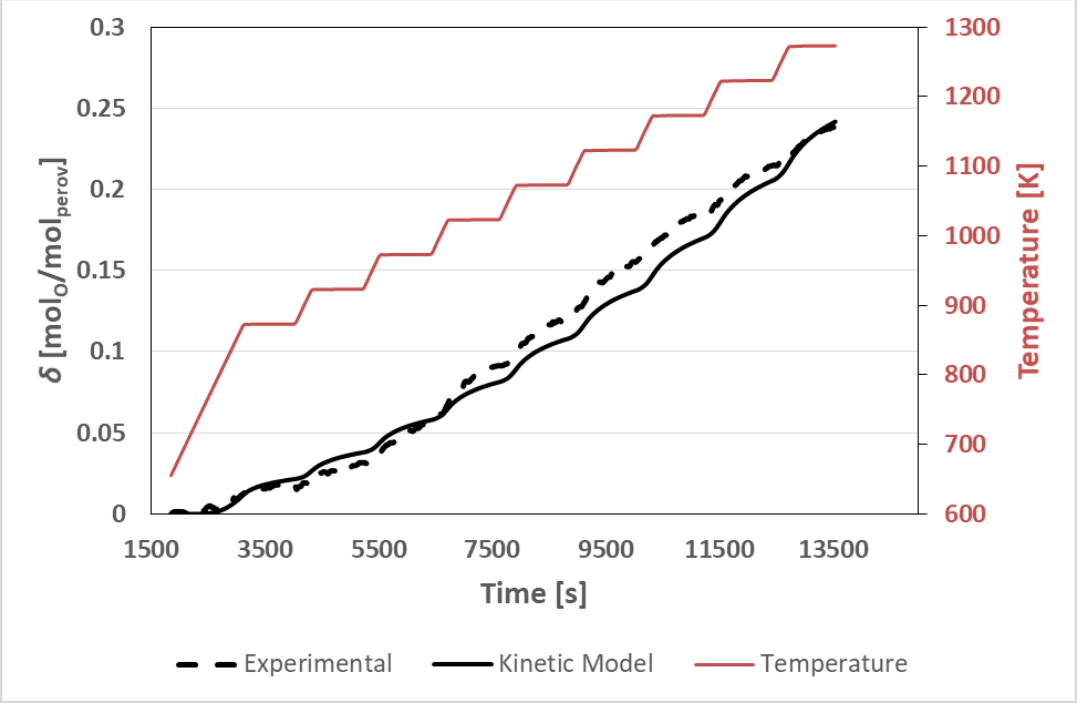

Figure 2: Kinetic model predictions compared to TGA measurements for CS10MO reduction by stepwise heating under nitrogen flow

4.2 Oxidation kinetic parameters

Given the reduction kinetic parameters, the oxidation part of the same TGA experiment was analyzed in order to estimate the corresponding oxidation kinetic parameters.

In Figure 1, a drastic drop of the non-stoichiometry parameter, δ, is observed which took place exactly when the gas was switched from pure nitrogen to air. During the isothermal segments an equilibrium value of δ is reached, as inferred from the shape of the δ curve that becomes practically parallel to the x-axis, in contrast to the respective reduction curve segments. Further, in the first repetition, δ approaches zero when cooling down to a temperature of 873 K (600°C). However, in the second repetition δ values show as negative; close to -0.03. This difference is pretty steady throughout the complete oxidation of the second repetition and it is argued that it results from the instrument measurement drift. Therefore, for the oxidation analysis the first oxidation step was taken into consideration.

The resulting parameters for the oxidation reaction are $k_{0,ox} = 2 \cdot 10^{14}\, s^{-1}$, $E_{A,0,ox} = 267500\, J\, mol^{-1}$, $c_{ox} = -400000\, J\, mol^{-1}$ and $\delta \exp_{ox} = 0.63$. In Figure 3, the comparison of the model results with data from the TGA experiment is presented.

It has to be noted that it may be counterintuitive for the c_{ox} to be negative. The most possible explanation is that the reduction parameters have been estimated based on experiments with pure nitrogen assuming that absolutely no oxygen is present in the reaction chamber and only the reduction reaction is taking place. However, it is possible that limited presence of oxygen due to both continuous reduction of the material and insufficient instantaneous removal of it from the reaction chamber in

combination with potential minor diffusional air leakages from the environment directly affect the reduction kinetics parameter estimation. This claim is enhanced by the very high sensitivity of the material to oxygen traces, which has already been demonstrated and analyzed via experimental results provided in deliverable D2.1. In any case, the kinetic parameters applied do model the macroscopic perovskite behavior during various experimental process conditions, as it is presented in the following sections.

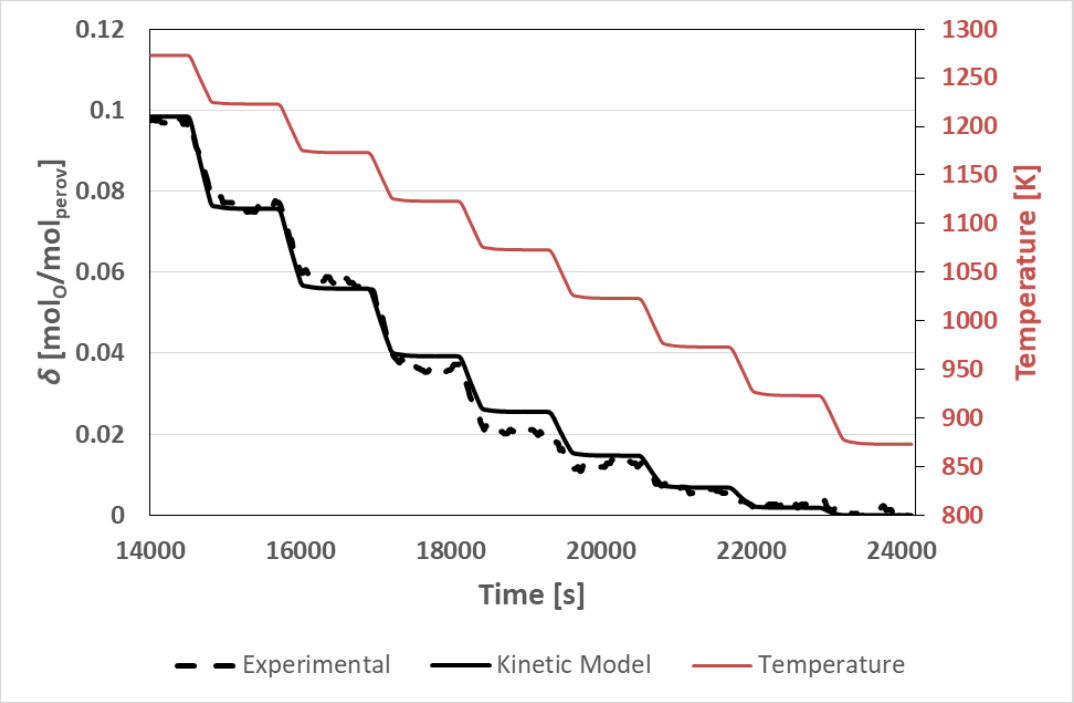

Figure 3 Kinetic model predictions compared with TGA measurements for CS10MO oxidation by stepwise cooling under air flow

5 Redox kinetic model validation

Following the parameter estimation procedure, the model was compared to the results of experiments under different operating conditions so as to validate its performance. The kinetic parameters estimated and used for the model validation procedure are summed up in Table 1.

Table 1: Kinetics parameters of the CS10MO redox reaction as estimated and applied to the model

Reduction reaction				Oxidation reaction				
$k_{0,red}$ [s^{-1}]	$E_{A,0,red}$ [J mol^{-1}]	c_{ox} [J mol^{-1}]	δexp_{red} [-]	$k_{0,ox}$ [s^{-1}]	$E_{A,0,ox}$ [J mol^{-1}]	c_{ox} [J mol^{-1}]	δexp_{ox} [-]	$yexp$ [-]
$3.05 \cdot 10^{17}$	332000	492000	0.6	$2 \cdot 10^{14}$	267500	-400000	0.63	1

Experiments in the purpose-built test-rig were simulated for three different operation protocols; (a) perovskite reduction by step-wise heating, (b) perovskite reduction by continuous heating and (c) perovskite oxidation by continuous cooling. Relevant details are included in submitted deliverable D2.1. All three operation protocols were carried out under air flow with $Y_{ox} = 0.21$, at an operating pressure of 1 bar and within the temperature range of 950 to 1400 K (~ 700-1100°C). It is important

to mention that, in the test rig experiments considered here, a small-scale honeycomb CS10MO perovskite structure (of 59 cpsi geometry as analyzed in D2.1) was used, which is a scaled-down version of the most possible candidate towards pilot scale experiments based on current project findings and in alignment with the initial project's target for redox structured bodies utilization. The model results from the three operation protocols are compared to the respective experimental measurements and presented in Figure 4, Figure 5 and Figure 6.

In the operation protocol (a), at low temperatures, a good prediction of the δ values is noticed. This is true even at the very low temperatures of approximately 700 K, measured during the initial heating up of the structure from room temperature (i.e. 1st reduction step). Therefore, the model can provide reliable results at low temperatures. At high temperatures, the model also provides good predictions of the non-stoichiometry parameter. At medium temperatures, i.e. 1100-1300 K, the model slightly underestimates the experimental results. However, this error is not considered significant and is measured to be less than 13%.

In the operation protocol (b), at temperatures from 970 K to 1280 K, the model reproduces the behavior of the perovskite redox reaction, except for the time when the temperature starts to increase, in which the model overestimates the result. At temperatures over 1280 K, the model also starts to deviate from the experimental ones. These over-predictions are most likely caused by the temperature differences of the perovskite structure due to thermal gradients, which were not considered by the model and were also not technically feasible to be measured experimentally. This can be proven by the operating protocol (a) estimations, in which the temperature is raised gradually, thereby providing more time for the structure to achieve a relatively more homogeneous temperature profile.

In the operation protocol (c), model behavior is observed to be similar to protocol (b). At temperatures over 1300 K, it overestimates the results for the same reason described in the previous paragraph. At temperatures below 1150 K, the model starts to deviate from the experimental measurements. This may result from the structure thermal gradients and the technical difficulty to measure low oxygen amounts consumed, as it has already been discussed.

Overall, the model seems to make good predictions of the non-stoichiometry values. Further kinetic studies will be conducted, during the course of project, performing coupled CFD, thermal and redox reaction simulations. In such simulations the thermal gradients will be calculated and in turn taken into consideration providing better insight into the redox kinetic model ability to predict perovskite behavior.

It has to be noted that in operation protocol (b) and (c), the experimental results were offset by 0.005. This offset was applied to match the experimental value at the beginning of the experiment, due to the same technical difficulties in experimental measurement of δ value at low temperatures.

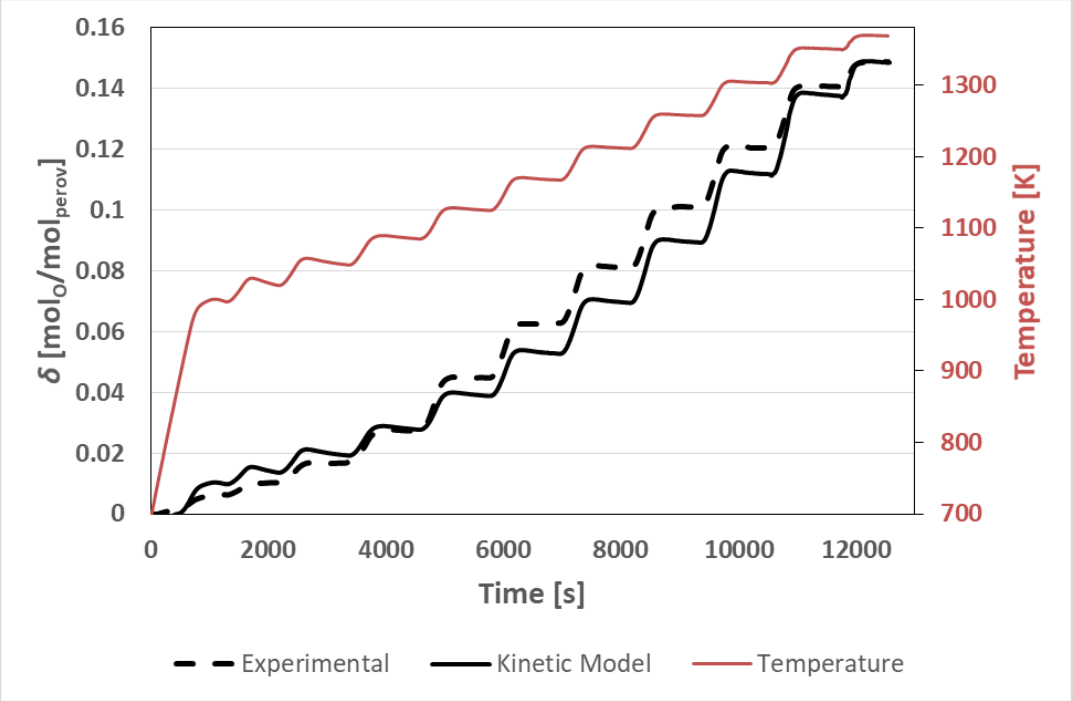

Figure 4: Kinetic model predictions compared with experimental measurements produced from the purpose-built test-rig for the CS10MO structure reduction by stepwise heating under air flow (protocol (a))

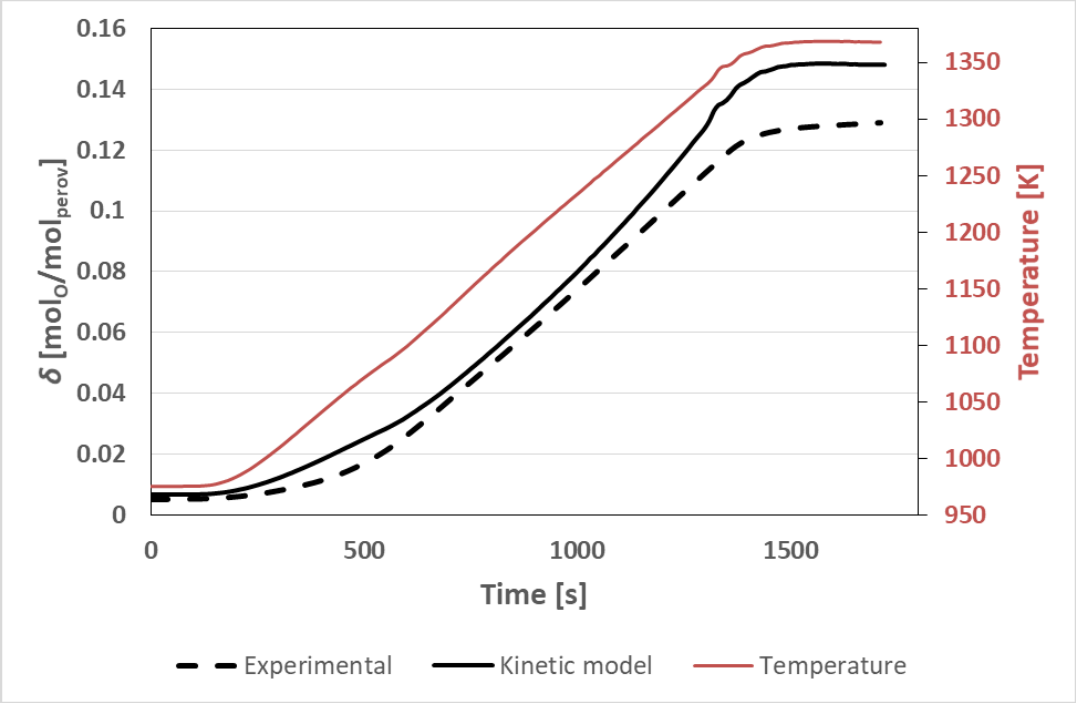

Figure 5: Kinetic model predictions compared with experimental measurements produced from the purpose-built test-rig for the CS10MO structure oxidation by continuously heating under air flow (protocol (b))

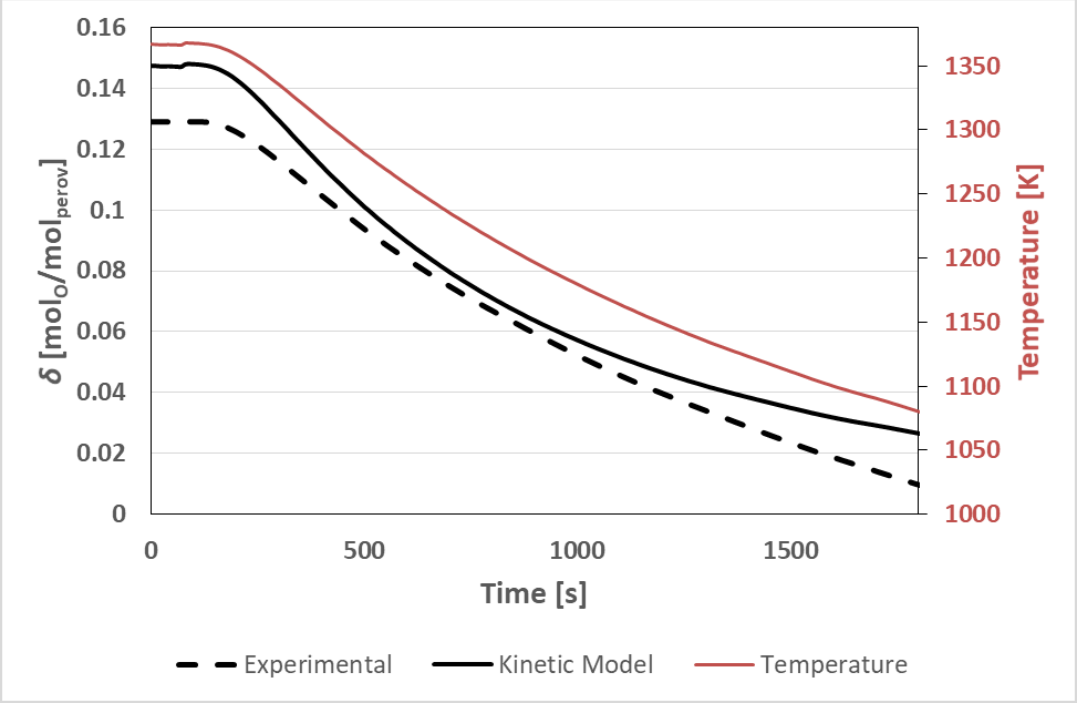

Figure 6: Kinetic model predictions compared with experimental measurements produced from the purpose-built test-rig for the CS10MO structure oxidation by continuously cooling under air flow (protocol (c))

6 Conclusions and next steps

In Task 2.4, a reduction-oxidation model was developed to simulate the perovskite kinetic behavior during operation. The modeling activities were focused on developing a theoretical approach with physical and chemical meaning. A model was formulated based on a phenomenological approach that includes a reduction and an oxidation reaction that follow the Arrhenius law, in which oxygen concentration and non-stoichiometry level effects have been taken into consideration. Certain modifications have been introduced based on the experimental behavior of the redox material.

The innovation of this task is that although the described theoretical approach is highly based on a well-known chemical law, it has not been expressed within the literature as such for this kind of applications. Provided that this model is able to be verified and validated against multiple process conditions (a process currently in progress), it may provide insight on the perovskite behavior in similar applications. Although the first results are positive and show clear potential, further study and experiments are required to establish the performance of this approach for a wide range of process conditions.

A redox kinetic parameters estimation procedure was followed using TGA data and optimization functions. The TGA data are comprised of two operating protocols; a reduction by a stepwise temperature increase under inert atmosphere and an oxidation by a stepwise decrease of temperature under air.

Towards model validation, the developed model was applied to predict δ values from the experiments with the purpose-built test-rig carried out at three additional operating protocols; a reduction by stepwise increase of temperature, a reduction by continuously increasing temperature and an oxidation by continuously decreasing temperature. All experiments analyzed were carried out using a constant air flow at pressure of 1 bar.

The results from the comparison of the model predictions and experimental measurements indicated that the model is able to simulate the perovskite behavior during redox operation. More specifically, the model performed well at low (700 to 1100 K) and high (1300-1400 K) temperatures, while at medium temperature the error of δ estimations did not exceed 15%.

Important findings are going to be produced from the planned experiments during the next months of the project. Such experiments will be at TGA- lab- (WP1, WP2) and pilot-scale (WP4). This data will be used to further develop, refine and verify the perovskite redox kinetic model. Model developments and results will be presented in the 2nd periodic report of the project.

References

Bulfin, B., Vieten, J., Richter, S., M. Naik, J., R. Patzke, G., Roeb, M., Sattler, C., Steinfeld, A., 2020. Isothermal relaxation kinetics for the reduction and oxidation of SrFeO 3 based perovskites. Phys. Chem. Chem. Phys. 22, 2466–2474. https://doi.org/10.1039/C9CP05771D

de Diego, L.F., Abad, A., Cabello, A., Gayán, P., García-Labiano, F., Adánez, J., 2014. Reduction and Oxidation Kinetics of a CaMn0.9Mg0.1O3−δ Oxygen Carrier for Chemical-Looping Combustion. Ind. Eng. Chem. Res. 53, 87–103. https://doi.org/10.1021/ie4015765

Go, K.S., Son, S.R., Kim, S.D., 2008. Reaction kinetics of reduction and oxidation of metal oxides for hydrogen production. Int. J. Hydrog. Energy 33, 5986–5995. https://doi.org/10.1016/j.ijhydene.2008.05.039